

On the composition of the crystal phases in the PbO-TeO₂ system

D. STAVRAKIEVA, Y. IVANOVA
Higher Institute of Chemical Technology, 1756 Sofia, Bulgaria

J. PYROV
Scientific Manufacturing Enterprise of Electrothermics, 1870 Sofia, Bulgaria

The phase diagrams and the inconsistencies in the type and composition of the crystal phases in the PbO-TeO₂ system reported by different workers are reported. With the help of X-ray microanalysis, X-ray analysis and IR spectroscopy new data about the composition of the crystal phases have been obtained. The data from the X-ray microanalysis were treated by the method of the number of the oxygen atoms, and the chemical formulae of the crystal phases were evaluated. The following phases were established: solid solution from PbO · 4TeO₂ in 2PbO · 7TeO₂, 2PbO · 5TeO₂, 2PbO · 3TeO₂, PbO · TeO₂ with two polymorphic modifications, a phase with varied composition from 5PbO · 2TeO₂ to 3PbO · TeO₂, and 5PbO · TeO₂. It was assumed that there was polymorphic transformation for the 2PbO · TeO₂, 3PbO · TeO₂ and 5PbO · TeO₂ compositions. Data from X-ray analysis and the IR absorption spectra are presented. On the basis of the new data for the composition of the crystal phases and the data from the investigations of different workers a corrected phase picture of the PbO-TeO₂ system is built up.

1. Introduction

The PbO-TeO₂ system has been the object of a number of investigations. The thermal resistance of PbTeO₃ and PbTeO₄ was investigated by Tananaeva and Novoselova [1]. The polymorphic transformation of PbO · TeO₂ compound, melting with decomposition at 560°C and forming a phase richer in lead (Pb/Te = 1.08), was determined. The system was investigated by Marinov *et al.* [2] in the range from 0 to 50 mol % PbO. Crystal phases with PbO · 4TeO₂, PbO · 2TeO₂, 2PbO · 3TeO₂ and PbO · TeO₂ composition were established and the polymorphic transformation of PbO · TeO₂ was confirmed. The morphological characteristics were described and the interplanar spacings were determined. A phase picture of the PbO-TeO₂ system in the concentration range from 0 to 50 mol % PbO (Fig. 1)

was built up. Later, Robertson *et al.* [3] confirmed the PbO · 3TeO₂ phase, but they did not verify the formation of PbO · TeO₂. They determined 3PbO · TeO₂ and 6PbO · TeO₂ phases and constructed the phase picture of the system for the range from 0 to 100 mol % PbO (Fig. 2). The same workers [3] presented the phase diagram of the PbO-TeO₂ system after Cole and Douglas (Fig. 3) which was not previously reported. The investigations of Young [4] in the same system in an atmosphere of argon in the range 40 to 75 mol % PbO showed a different course of the liquidus line (Fig. 4). It was confirmed that there was formation of 2PbO · 3TeO₂ and PbO · TeO₂ with polymorphic transformation at 665 ± 2°C, melting incongruently at 690 ± 3°C. Kosse and collaborators [5, 6] have synthesized PbO · TeO₂ (tetrahedral),

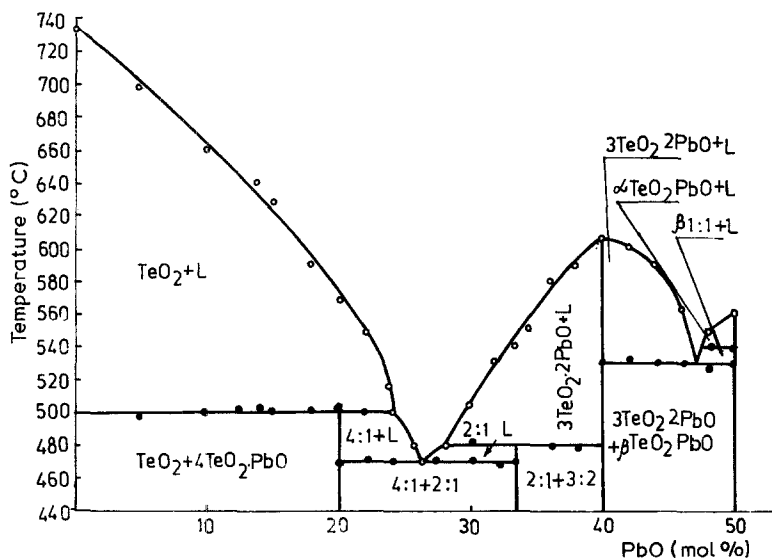


Figure 1 Phase diagram of the PbO-TeO₂ system after Marinov *et al.* [2]. L = liquid.

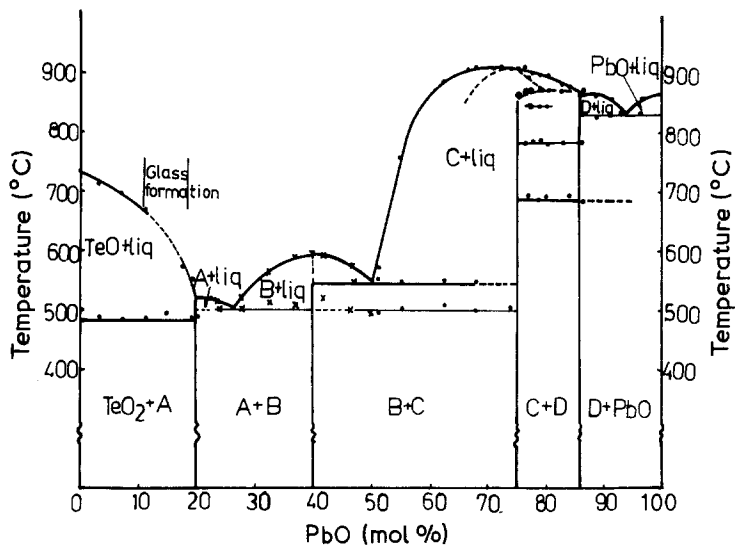


Figure 2 Phase diagram of the PbO-TeO₂ system after Robertson *et al.* [3]. A = PbO · 4TeO₂, B = 2PbO · 3TeO₂, C = 3PbO · TeO₂ or 8PbO · 3TeO₂, and D = 6PbO · TeO₂.

Figure 3 Phase diagram of the PbO-TeO₂ system after Cole and Douglas (1964, unpublished) from Robertson *et al.* [2]. A = 4TeO₂ · PbO, B = 3TeO₂ · 2PbO and C = TeO₂ · 4PbO.

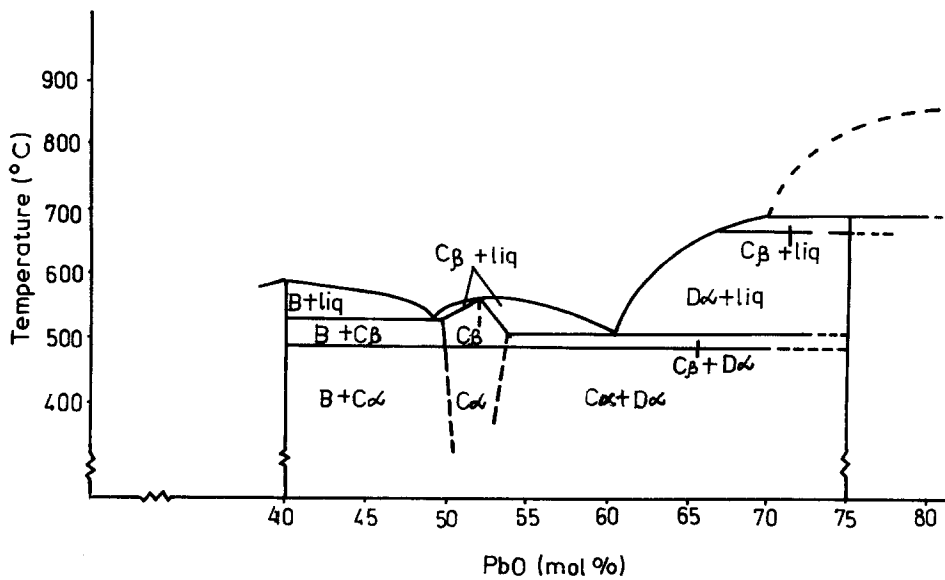
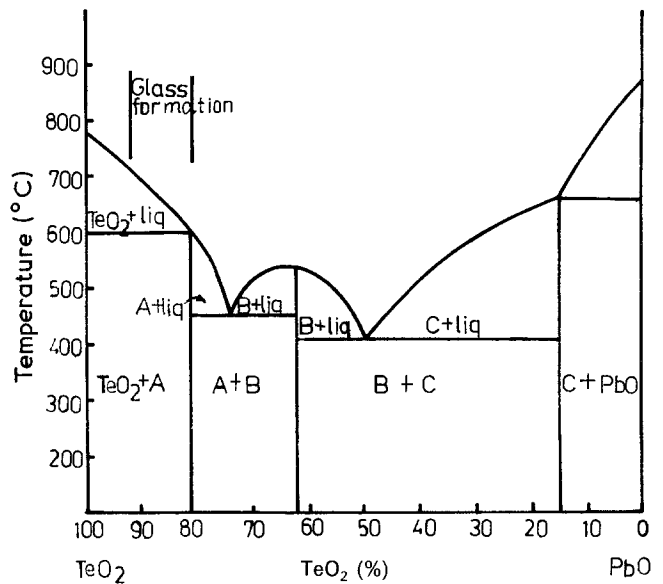


Figure 4 Central part of the PbO-TeO₂ system after Young [4]. B = Pb₂Te₃O₃, C = PbTeO₃, D = Pb₃TeO₃.

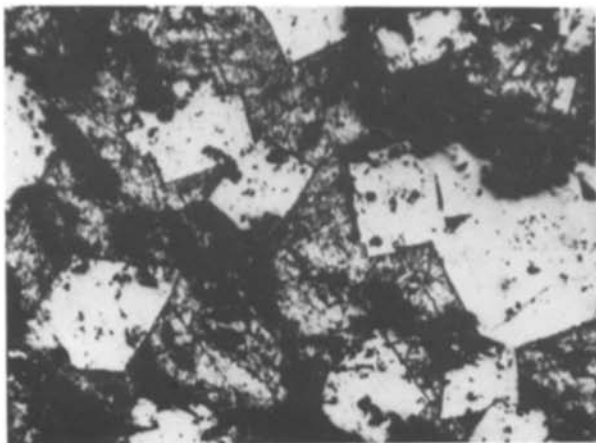


Figure 5 Idiomorphic crystals of $\text{PbO} \cdot 4\text{TeO}_2$. Reflected light. Crystals etched by dilute HCl. Magnification $139\times$.

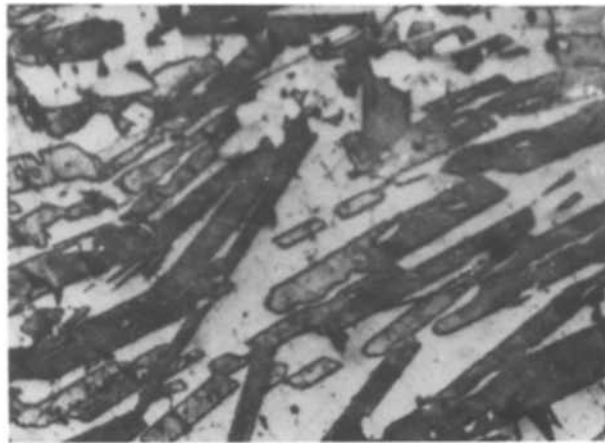


Figure 7 Elongated rhombic sections of $2\text{PbO} \cdot 3\text{TeO}_2$. Reflected light. Etched by dilute HCl. Magnification $139\times$.

Pb_3TeO_5 and Pb_3TeO_6 by slow cooling of the melt and single crystals of PbTeO_3 (monoclinic) as well as $\text{Pb}_2\text{Te}_3\text{O}_8$ by the method of Chochralsky, and they have examined their dielectric properties. They confirmed that PbTeO_3 (tetrahedral) and Pb_3TeO_6 had undergone reversible phase transformations at 530 and 490 K, respectively, and at the temperature of the phase transformation they were in a spontaneously polarized state, determining them as ferroelectrics.

The aim of the present work is to explain the composition of the newly forming crystal phases in the system $\text{PbO}-\text{TeO}_2$ because of the contradictions in the investigations by the workers mentioned above.

2. Experimental procedure

Samples corresponding to the stoichiometric ratios of $\text{PbO} \cdot 4\text{TeO}_2$, $\text{PbO} \cdot 2\text{TeO}_2$, $2\text{PbO} \cdot 3\text{TeO}_2$, $\text{PbO} \cdot \text{TeO}_2$, $2\text{PbO} \cdot \text{TeO}_2$, $3\text{PbO} \cdot \text{TeO}_2$, $4\text{PbO} \cdot \text{TeO}_2$ and $6\text{PbO} \cdot \text{TeO}_2$ were synthesized by crystallization at temperatures above the solidus temperatures (in the range between solidus and liquidus). The operating conditions are presented in Table I. The thermal treatment of the samples was performed in air. The synthesis was followed by the X-ray technique (apparatus by DRON, powder samples, $\text{CuK}\alpha$ radiation). The IR spectra were taken on a Karl Zeiss Jena UR-10 spectrometer (1400 to 700 cm^{-1} with NaCl prism, 700 to 400 cm^{-1} with KBr prism). The samples were prepared as tablets with KBr. TeO_2 (USSR) and Pb_3O_4 were

used as starting materials. The composition of the crystal phases was determined with the help of an X-ray microanalyser (Philips). In order to avoid casual mistakes the analyses were performed at points on at least 5 to 6 different crystal specimens, as well as on the glassy state. The data obtained were treated with a microprocessor.

3. Results and discussion

In Figs 5 to 12 the morphologies of the crystal phases at the analysed points are given. The results of the chemical analyses by using electron microscopy were used to derive crystallochemical formulae based on the number of oxygen atoms. In Table I the compositions in accordance with the data from X-ray

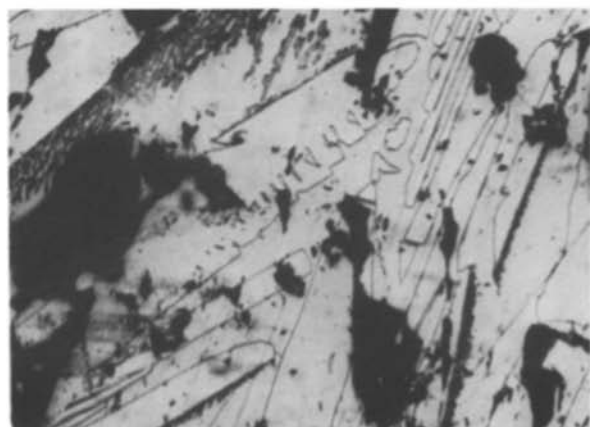


Figure 6 Prismatic crystals of $2\text{PbO} \cdot 5\text{TeO}_2$. Reflected light. Magnification $139\times$.

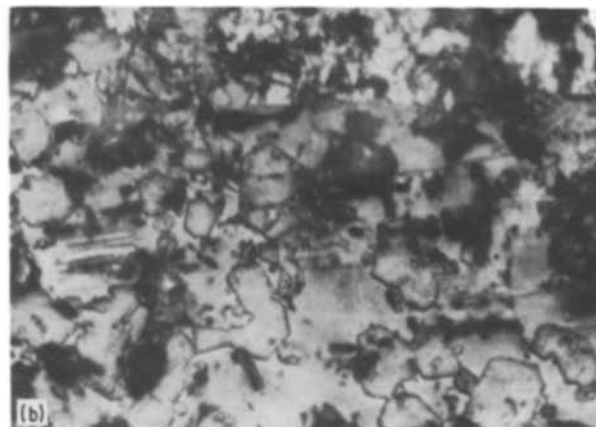
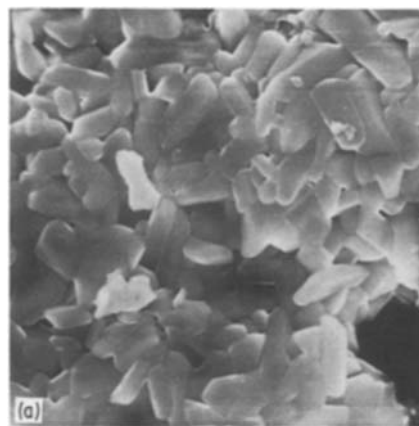


Figure 8 Single crystals of the $\text{PbO} \cdot \text{TeO}_2$ phase: (a) scanning electron microscopy, $310\times$; (b) reflected light, $139\times$.

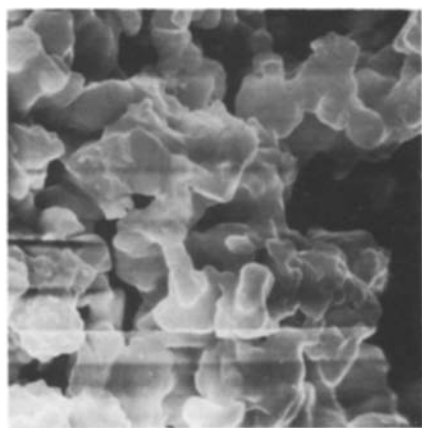


Figure 9 Mass crystallization of crystals of $2\text{PbO} \cdot \text{TeO}_2$. Scanning electron microscopy. Magnification $310 \times$.

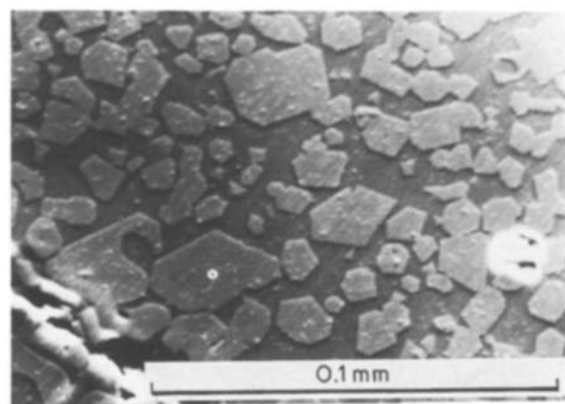


Figure 11 Analysed crystals of the $3\text{PbO} \cdot \text{TeO}_2$ phase from $4\text{PbO} \cdot \text{TeO}_2$ composition. Scanning electron microscopy. Magnification $485 \times$.

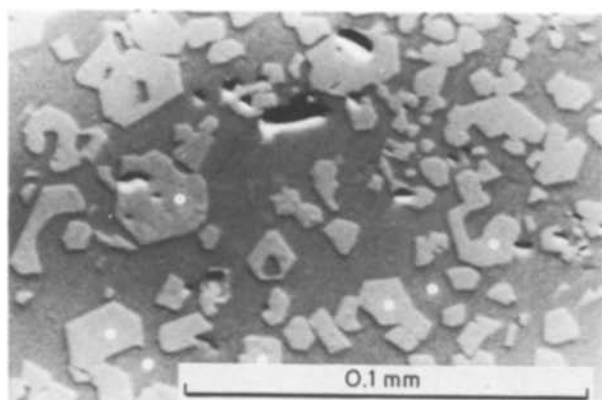


Figure 10 Analysed crystals of the $3\text{PbO} \cdot \text{TeO}_2$ phase. Magnification $485 \times$. Scanning electron microscopy.

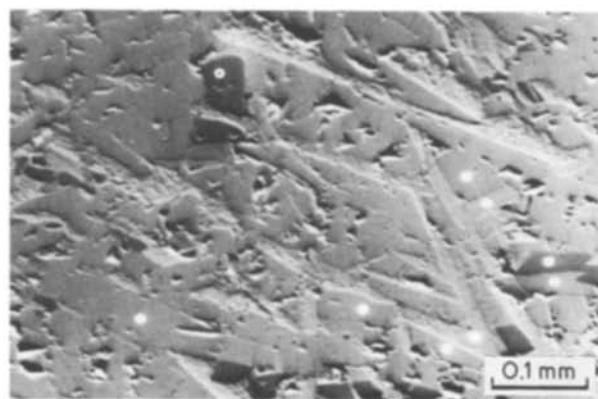


Figure 12 Analysed crystals of the $5\text{PbO} \cdot \text{TeO}_2$ phase from $6\text{PbO} \cdot \text{TeO}_2$ composition. Electron scanning microscopy. Magnification $115 \times$.

microanalysis are presented. Data from X-ray microanalysis in the investigated concentration range confirm the formation of phases with $3\text{PbO} \cdot 2\text{TeO}_2$ composition. New crystal phases with $2\text{PbO} \cdot \text{TeO}_2$ and $5\text{PbO} \cdot \text{TeO}_2$ composition were determined. The existence of polymorphic forms of the $5\text{PbO} \cdot \text{TeO}_2$ phase was assumed. Samples with a stoichiometric ratio $3\text{PbO} \cdot \text{TeO}_2$ correspond to a phase with variable composition from $5\text{PbO} \cdot 2\text{TeO}_2$ to $3\text{PbO} \cdot \text{TeO}_2$ (from 61.5 to 75 mol % PbO, respectively), probably with polymorphic transformation. For samples corresponding to the stoichiometric ratio $\text{PbO} \cdot 2\text{TeO}_2$, thermally treated above 470°C , we identified a $2\text{PbO} \cdot 3\text{TeO}_2$ phase, and below the above-mentioned temperature

crystal phases of the $2\text{PbO} \cdot 5\text{TeO}_2$ and $2\text{PbO} \cdot 3\text{TeO}_2$ type were both present. Consequently, the X-ray data given by Marinov *et al.* [2] for $\text{PbO} \cdot 2\text{TeO}_2$ composition correspond to a crystal phase with composition $2\text{PbO} \cdot 5\text{TeO}_2$ composition.

At $\text{PbO} \cdot 4\text{TeO}_2$ stoichiometric ratio the identified crystal phase has a variable composition from 20 to 22.2 mol % PbO, corresponding to $4\text{TeO}_2 \cdot \text{PbO}$ to $7\text{TeO}_2 \cdot 2\text{PbO}$, respectively, and X-ray data given by Marinov *et al.* [2] correspond to this phase. On the basis of the results from X-ray microanalysis the interplanar spacings of the crystal phases are as summarized in Table II.

The characteristic IR absorption spectra of the

TABLE I Composition of crystal phases in the $\text{PbO}-\text{TeO}_2$ system

Phase No.	Given stoichiometric composition	Composition of the crystal phases from X-ray microanalysis data	Figure	Temperature of crystallization ($^\circ\text{C}$)
1	$\text{PbO} \cdot 4\text{TeO}_2$	$(2\text{PbO} \cdot 7\text{TeO}_2$ to $\text{PbO} \cdot 3\text{TeO}_2)$	5	480
2	$\text{PbO} \cdot 2\text{TeO}_2$	solid solution + $2\text{PbO} \cdot 5\text{TeO}_2$ $2\text{PbO} \cdot 5\text{TeO}_2$ + $2\text{PbO} \cdot 3\text{TeO}_2$ $2\text{PbO} \cdot 3\text{TeO}_2$ + glassy phase	6	Below 470 Above 470 (crystallization from the melt)
3	$2\text{PbO} \cdot 3\text{TeO}_2$	$2\text{PbO} \cdot 3\text{TeO}_2$	7	580
4	$\text{PbO} \cdot \text{TeO}_2$	$\text{PbO} \cdot \text{TeO}_2$	8	540
5	$2\text{PbO} \cdot \text{TeO}_2$	$2\text{PbO} \cdot \text{TeO}_2$	9	550
6	$3\text{PbO} \cdot \text{TeO}_2$	$(3\text{PbO} \cdot \text{TeO}_2$ to $5\text{PbO} \cdot 2\text{TeO}_2)$	10	670
7	$4\text{PbO} \cdot \text{TeO}_2$	solid solutions $3\text{PbO} \cdot \text{TeO}_2$	11	670
8	$6\text{PbO} \cdot \text{TeO}_2$	$5\text{PbO} \cdot \text{TeO}_2$	12	840

TABLE II X-ray data for the phases in PbO-TeO₂

PbO · 4TeO ₂ to 2PbO · 7TeO ₂ (s.s.) Orthorhombic [2]*		2PbO · 5TeO ₂ Monoclinic [2]*		2PbO · 3TeO ₂ Orthorhombic [3] <i>a</i> = 0.714 nm, <i>b</i> = 1.877 nm, <i>c</i> = 1.945 nm Interplanar spacings [2, 4]*		PbO · TeO ₂ Monoclinic [2, 4] <i>a</i> = 2.759 nm, <i>b</i> = 0.461 nm, <i>c</i> = 1.797 nm, β = 112.90° [4] Interplanar spacings [1, 2, 4]*		PbO · TeO ₂ Tetragonal [4] <i>a</i> = 0.533 nm, <i>c</i> = 1.188 nm, [4]; <i>a</i> = 0.5323 ± 0.0002 nm, <i>c</i> = 1.1950 ± 0.0008 nm, 14 ₁ md [5] Interplanar spacings [1, 2, 4, 5]*		2PbO · TeO ₂ [†] Monoclinic (?)		β -3PbO · TeO ₂ (s.s.) [†] Orthorhombic [6] <i>a</i> = 0.55 nm, <i>b</i> = 0.66 nm, <i>c</i> = 1.15 nm [6]		α -3PbO · 2TeO ₂ to 3PbO · TeO ₂ (s.s.) [†] Orthorhombic [6] <i>a</i> = 0.55 nm, <i>b</i> = 0.66 nm, <i>c</i> = 1.15 nm [6]		5PbO · TeO ₂ [†]	
<i>I</i>	<i>d</i> (nm)	<i>I</i>	<i>d</i> (nm)	<i>I</i>	<i>d</i> (nm)	<i>hkl</i>	<i>I</i>	<i>d</i> (nm)	<i>hkl</i>	<i>I</i>	<i>d</i> (nm)	<i>I</i>	<i>d</i> (nm)	<i>I</i>	<i>d</i> (nm)	<i>I</i>	<i>d</i> (nm)
35	0.339	5	0.342	m	0.979	002	w	0.839	002	5	0.4864	101	0.507	4	0.374	9	0.375
100	0.324	70	0.317	vw	0.545	211	w	0.635	402	100	0.3184	112	0.313	33	0.342	11	0.342
20	0.310	100	0.307	w	0.488	004	w	0.355	013	16	0.2987	004	0.306	100	0.339	53	0.323
70	0.298	5	0.294	w	0.470	400	w	0.347	413	90	0.2658	200	0.300	68	0.322	5	0.313
20	0.280	3	0.288	w	0.431	204	vw	0.331	701	4	0.2338	211	0.285	32	0.304	27	0.305
12	0.239	2	0.270	w	0.431	204	vw	0.331	701	2	0.2180	105	0.271	100	0.298	100	0.299
15	0.1985	2	0.252	vw	0.385	411	s	0.323	314	3	0.2042	213	0.218	19	0.218	83	0.296
20	0.1866	2	0.240	vw	0.350	120	s	0.311	705	26	0.1987	204	0.2108	31	0.283	11	0.284
23	0.1692	2	0.230	s	0.330	122	s	0.300	406	12	0.1881	220	0.2088	3	0.279	17	0.280
6	0.1650	2	0.218	s	0.322	215	s	0.286	901	12	0.1759	116	0.1806	20	0.272	2	0.265
2	0.1555	3	0.2005	vs	0.311	320	mw	0.286	710	1	0.1684	215	0.1768	21	0.265	3	0.255
4	0.1509	5	0.1825	s	0.300	602	mw	0.273	811	29	0.1619	312	0.1733	14	0.255	13	0.218
2	0.1486	2	0.1788	mw	0.284	315	w	0.266	806	17	0.1591	224	0.1684	21	0.253	32	0.210
10	0.1473	2	0.1765	mw	0.284	420	mw	0.253	206	3	0.1491	008	0.1675	20	0.241	5	0.203
		5	0.1702	s	0.276	611	ms	0.230	020	4	0.1391	217	0.1565	6	0.218	5	0.1996
		3	0.1690	s	0.260	124	mw	0.226	406	6	0.1333	400	0.1530	16	0.214	6	0.1966
		5	0.1578	vw	0.260	224	mw	0.221	617	10	0.1303	208	0.1501	10	0.212	6	0.1939
		2	0.1553	vw	0.260	017	vw	0.218	804	19	0.1285	316	0.1428	4	0.210	2	0.1840
				m	0.253	515	ms	0.211	017	9	0.1382	6	0.1382	9	0.203	8	0.1768
				vw	0.241	317	ms	0.186	824	8	0.1371	6	0.1371	8	0.1993	8	0.1760
				vw	0.234	131	m	0.182	426	8	0.1367	5	0.1367	8	0.1986	2	0.1730
				w	0.228	417	m	0.179	408	9	0.1346	6	0.1346	14	0.1965	14	0.1715
				w	0.223	033	w	0.177	1022	5	0.1330	5	0.1330	8	0.1934	8	0.1691
				vw	0.215	720	mw	0.173	10010	3	0.1290	5	0.1290	5	0.1859	8	0.1621
				s	0.210	333	mw	0.168	127			5		6	0.1839	6	0.1616
				s	0.202	219						8		8	0.1764	6	0.1480
				s	0.194	0010						11		11	0.1758	4	0.1464
				m	0.180	920						8		8	0.1741	26	0.1666
				m	0.178	140						15		15	0.1712	17	0.1601
				m	0.169	808						6		6	0.1688	9	0.1578
				s	0.165	3210						10		10	0.1641	5	0.1527
				m	0.161	540						5		5	0.1616		
				w	0.157	542											
				w	0.152	1017											

* Interplanar spacings from corresponding reference.

† Interplanar spacings from current work.

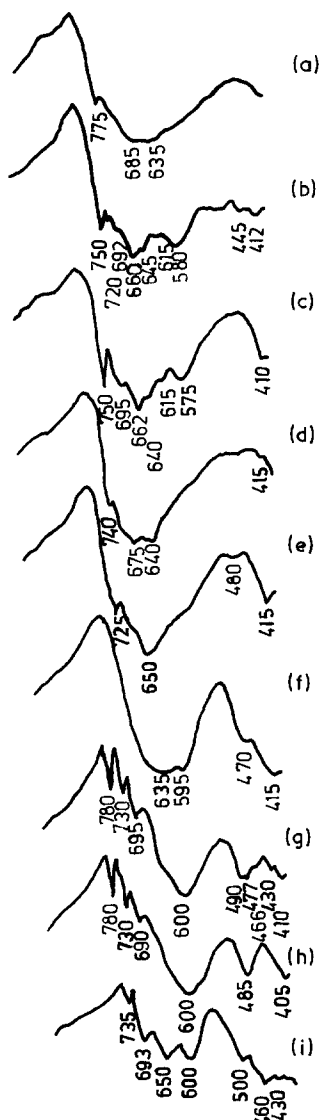


Figure 13 Infrared absorption spectra (cm^{-1}) of crystal phases from the $\text{PbO}-\text{TeO}_2$ system: (a) $\text{PbO} \cdot 4\text{TeO}_2$, (b) $2\text{PbO} \cdot 5\text{TeO}_2$, (c) $2\text{PbO} \cdot 3\text{TeO}_2$, (d) $\beta\text{-PbO} \cdot \text{TeO}_2$, (e) $\alpha\text{-PbO} \cdot \text{TeO}_2$, (f) $2\text{PbO} \cdot \text{TeO}_2$, (g) $\beta\text{-}3\text{PbO} \cdot \text{TeO}_2$, (h) $\alpha\text{-}3\text{PbO} \cdot \text{TeO}_2$ and (i) $5\text{PbO} \cdot \text{TeO}_2$.

crystal phases in the $\text{PbO}-\text{TeO}_2$ system are shown in Fig. 13. The results obtained could be used for characterization of their structure.

4. Conclusion

With the help of X-ray microanalysis the composition of the newly forming phases in the binary $\text{PbO}-\text{TeO}_2$ system was examined. The formation of phases with $2\text{PbO} \cdot 3\text{TeO}_2$ composition was confirmed, and the phase $5\text{TeO}_2 \cdot 2\text{PbO}$ corresponds to the phase $2\text{TeO}_2 \cdot \text{PbO}$. The formation of new phases with chemical composition $2\text{PbO} \cdot \text{TeO}_2$, $5\text{PbO} \cdot \text{TeO}_2$ and two phases with variable composition $4\text{TeO}_2 \cdot \text{PbO}$ to $7\text{TeO}_2 \cdot 2\text{PbO}$ (from 20 to 22.2 mol % PbO) and $5\text{PbO} \cdot 2\text{TeO}_2$ (from 61.5 to 75 mol % PbO) was established. Based on the results for the chemical compositions of the crystal phases obtained by us and with respect to those reported by other workers, especially by Robertson and Young on temperature data in the range 50 to 100 mol % PbO for the course of the liquidus–solidus lines, a corrected phase diagram for the $\text{PbO}-\text{TeO}_2$ system (Fig. 14) was constructed.

References

1. O. I. TANANAIEVA and A. N. NOVOSELOVA, *Izv. Akad. Nauk USSR Neorg. Mater.* 3(1) (1967) 114.
2. M. R. MARINOV, R. G. SVESHTAROVA, D. A. STAVRAKIEVA and Y. B. DIMITRIEV, *C. R. Acad. Bulg. Sci.* 27(11) (1974) 1533.
3. D. S. ROBERTSON, N. SHAW and I. M. YOUNG, *J. Phys. D., Appl. Phys.* 9 (1976) 1257.
4. I. M. YOUNG, *J. Mater.* 14 (1979) 1579.
5. L. I. KOSSE, E. POLITOVA, A. A. BUSCH, A. V. ASTAFIEV and S. Y. STEFFANOVITCH, *J. Crystallogr.* 28(3) (1983) 510.
6. L. I. KOSSE, E. D. POLOTOVA, A. V. ASTAFIEV, A. B. GOURIEV, I. I. ZUTOK and Y. N. VENEVTZEV, *Physika Tverdogo Tela* 25(7) (1983) 2029.

Received 1 June

and accepted 27 July 1987

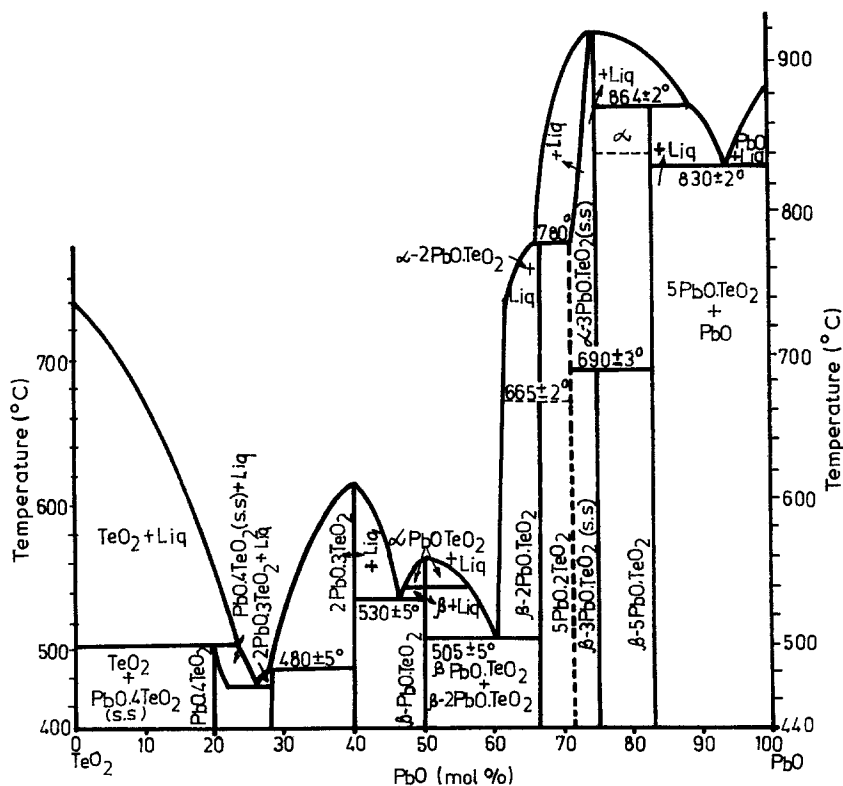


Figure 14 Phase diagram of the $\text{PbO}-\text{TeO}_2$ system from the current work.